Journal of Applied Technology and Innovation
Vol. **09,** Issue **2**, 2025**,** pp. **01-12**
e-ISSN:2600-7304-ISSN
DOI: https://doi.org/10.65136/jati.v9i2.10

Sliding Mode Control-Based Modeling and Analysis of Permanent Magnet DC Motors.

Ahmed Khamees [1*], Ashraf Alharam[1]

[1] College of Science and Technology, Umm Al-Aranib, Libya
*Corresponding Author: libya.ahmedsalihkhamees@gmail.com

Abstract

This paper developed a complete modeling and control framework for a permanent magnet direct current (PMDC) motor designs a first-order sliding mode control (SMC) with boundary-layer based on chattering reduction. The motor electrical and mechanical dynamics are derived in state-space form the equivalent-switching decomposition of SMC is obtained analytically. Simulation results in MATLAB/Simulink, under nominal and perturbed parameters, show that the proposed SMC archives an 86% reduction overshoot and 73% faster disturbance-recovery time significantly compared to a tuned PID controller. The controller is computationally simple and suitable for real-time implementation on low-cost DSPs platforms.

Keywords: *DC Motor, State-Space Modeling, Sliding Mode Control (SMC), Robustness, Chattering Reduction, Nonlinear Control.*

1. Introduction

Permanent magnet direct current (PMDC) motors are among the most frequently used actuators in modern electromechanical systems due to their simple structure, low cost, and excellent torque- speed characteristics. They are extensively used in robotics, electric vehicles, household appliances, medical devices, and automation systems. The ability of DC motors offers precise speed and position control makes them a preferred choice in applications requiring high dynamic performance (Fazdi & Hsueh, 2023; Shuraiji & Shneen, 2022). However, nonlinearities such as armature reaction, friction, load variation, and parameter uncertainties significantly affect the motor's dynamic response and steady-state accuracy (Afifa et al., 2023; Sengamalai et al., 2022). Therefore, robust control techniques are required to guarantee stable and efficient performance under various operating conditions.

The performance of DC motors has been the focus of extensive research, especially in the pursuit of advanced control strategies that overcome the limitations of classical methods such as proportional integral derivative (PID) control. While PID controllers remain popular due to simplicity and ease of implementation, they often exhibit limited robustness under parameter variations and external disturbances (Altinkaya et al., 2024; Parnianifard et al., 2018; Yaghoubi et al., 2025; Yusupov et al., 2023). Consequently, many modern intelligent control techniques have been developed to enhance system reliability, adaptability, and dynamic response. Active disturbance rejection control (ADRC) has emerged as a promising nonlinear control method for managing uncertainties and external disturbances. By incorporating elements such as tracking differentiators and extended state observers, ADRC effectively estimates and compensates for unknown dynamics, achieving better transient and steady-state performance in comparison with conventional PID control (Xu et al., 2023). Similarly, data-driven disturbance compensation approaches have gained attraction in recent years. These methods employ data-

driven disturbance observers to learn and model system behavior, allowing for real-time compensation of external disturbances. Experimental results have demonstrated that such methods keep strong control performance even in the presence of measurement noise and modeling inaccurate (Yue et al., 2023).

Another direction of research employs the uncertainty and disturbance estimation (UDE) technique, often combined with sliding mode control (SMC). The UDE-SMC framework improves robustness against nonlinearities such as friction and load torque variations while reducing the high-frequency chattering effect that traditionally limits SMC applications (Hu et al., 2021). SMC, itself has been extensively applied to DC motor systems due to its well-known robustness and simplicity in handling system uncertainties. Recent studies highlighted its capability to maintain stability and performance under wide operating condition (Mohd Zaihidee et al., 2019; Pan et al., 2017). Moreover, SMC offers fast dynamics response and superior transient behavior compared to PID and integral state feedback (ISF) controllers (Setiawan et al., 2025). However, the classical SMC approach suffers from chattering, a phenomenon caused by discontinuous control switching (Adamiak, 2020). To overcome this limitation, researchers have proposed hybrid and intelligent variants have been proposed such as fuzzy logic-based SMC, which adaptively tunes the switching gain and smooths control action, significantly mitigating chattering while maintaining robustness (Sahraoui et al., 2025; Tang & Ahmad, 2024). Comparative studies further confirm that SMC outperforms conventional controllers in reference tracking and disturbance rejection without overshoot, while fuzzy logic enhancements increase its adaptability and practical implementation (Yoganathan et al., 2024).

Despite the extensive research on DC motor control, few studies have presented a complete modeling-to-control framework that integrates physical modeling, state-space formulation, and sliding mode control design in a unified manner. Moreover, most existing works discuss SMC superficially without addressing chattering reduction methods or the mathematical formulation of the sliding surface design. There is still a lack of systematic comparison between theoretical modeling and practical control considerations for PMDC motors. The major contributions of this paper can be summarized as follows.

- Development of a complete dynamic model of a PMDC motor based on both electrical and mechanical differential equations.
- Derivation of the state-space representation and transfer function linking armature voltage to rotor speed and position.
- Design of a first-order SMC to achieve robust tracking performance under model uncertainties.
- Introduction of smooth approximation techniques to mitigate the chattering phenomenon in SMC.

Validation of the proposed framework using parameterized simulations to demonstrate improved speed regulation and robustness.

The rest of this paper is organized as follows. Section 2 deals with the mathematical modeling of the DC motor, including its physical and electrical characteristics, and state-space formulation. Section 3 describes the design and development of the sliding mode control strategy, including chattering mitigation techniques. Section 4 presents the simulation results and performance analysis of the proposed controller. Finally, Section 5 concludes the paper with remarks and recommendations for future work.

2. Methods

The proposed approach combines the dynamic modeling of a PMDC motor with a robust SMC strategy in order to achieve precise speed and position regulation under model uncertainties and external disturbances. The overall structure is divided into two broad sections: 1) Mathematical modeling and state-space formulation of PMDC motor dynamics, and 2) design of a first-order SMC law for robust nonlinear control with chattering mitigation.

2.1. DC Motor Modeling

The PMDC motor has an armature winding on the rotor and permanent magnets on the stator. The electromagnetic torque is proportional to the product of armature current and the magnetic flux. Figure1

illustrates the internal structure and torque generation mechanism. This figure depicts the important parts of the PMDC motor, which are the stator permanent magnets, rotor windings, commutator, and brushes. The magnetic interaction between the rotor current and the stator field produces electromagnetic torque, which drives the shaft rotation.

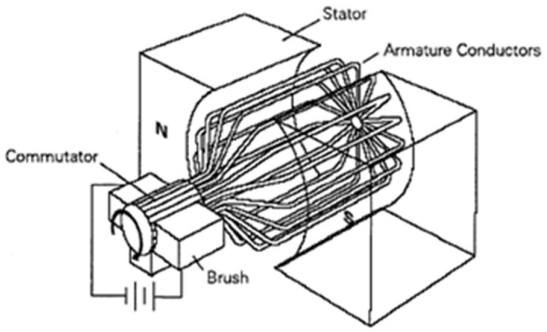

Figure 1. Illustration of a PMDC motor

2.2. Electrical and Mechanical Equations

To accurately analysis and control performance of a PMDC motor, it is necessary to first establish its fundamental electrical and mechanical equations. These equations describe the dynamic interactions between the electrical input, electromagnetic torque generation, and mechanical motion of the rotor form the basis for subsequent control system design and simulation. Applying Kirchhoff's Voltage Law (KVL) to the armature circuit gives:

$$V_a(t) = R_a i_a(t) + L_a \frac{di_a(t)}{dt} + e_b(t) \quad (1)$$

where, $V_a(t)$ is armature voltage (V) and $i_a(t)$ shows armature current (A). R_a represents armature resistance (Ω) and $L_a$indicates armature inductance (H). While $e_b(t)$ is back electromotive force (EMF) (V).

The back electromotive force (EMF) is proportional to the angular velocity:

$$e_b(t) = K_b \omega(t) \quad (2)$$

Here, $K_b$represents back EMF constant (V·s/rad), and $\omega(t)$ is angular speed (rad/s). The electromagnetic torque is expressed as:

$$T_m(t) = K_T i_a(t) \quad (3)$$

Where, K_T shows torque constant (N·m/A) and $T_m(t)$ is electromagnetic torque (N·m). The mechanical dynamics of the rotor, according to Newton's second law, are:

$$J_m \frac{d\omega(t)}{dt} + B_m \omega(t) = T_m(t) - T_L(t) \quad (4)$$

Where, $T_L(t)$ is load torque (N·m) and $J_m$represents rotor moment of inertia (kg·m²). Also, B_m is viscous friction coefficient (N·m·s/rad). Substituting (2) and (3) into (1) and (4) yields the coupled dynamics:

$$\begin{cases} V_a(t) = R_a i_a(t) + L_a \frac{di_a(t)}{dt} + K_b \omega(t) \\ K_T i_a(t) = J_m \frac{d\omega(t)}{dt} + B_m \omega(t) \end{cases} \quad (5)$$

Taking the Laplace transformation and eliminating $i_a(s)$, the transfer function between armature voltage and angular speed is obtained as:

$$\frac{\omega(s)}{V_a(s)} = \frac{K_T}{(L_a s + R_a)(J_m s + B_m) + K_T K_b} \quad (6)$$

The rotor position $\theta(s)$relates to angular speed by:

$$\theta(s) = \frac{1}{s}\,\omega(s) \tag{7}$$

The position-to-voltage transfer function (under no-load condition) can be derived similarly. When position is explicitly included, the resulting transfer function becomes third order. Figure 2 presents the electrical equivalent circuit of the PMDC motor, and the parameters with nominal values used in the simulations are listed in Table 1. The voltage drops across the armature resistance and inductance, together with the back-EMF, defines the electrical dynamics of the PMDC motor. These parameter values correspond to a small laboratory-scale PMDC motor commonly used in educational and experimental setups.

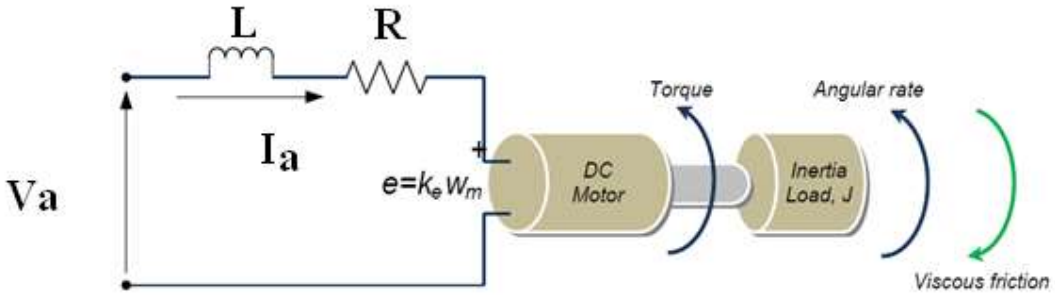

Figure 2. Electrical equivalent circuit of PMDC motor

Table 1. Motor parameters used for simulation

Parameter	Symbol	Value	Unit
Armature inductance	L_a	0.035	H
Armature resistance	R_a	2.45	Ω
Rotor inertia	J_m	0.022	kg·m²
Viscous friction	B_m	0.0005	N·m·s/rad
Torque constant	K_T	1.2	N·m/A
Back-EMF constant	K_b	1.2	V·s/rad

2.3. State-Space Representation

To facilitate controller design and performance analysis, the dynamic equations of the PMDC motor are reformulated in the state-space representation. Two common formulations are considered: (a) a two-state model (speed-current) and (b) an extended three-state model including the rotor position.

(a) Two-State Model (Speed and Current):

Let the state variables be defined as:

$$x_1 = \omega(t), \quad x_2 = i_a(t) \tag{8}$$

From Equation (5), the state-space equations are obtained as:

$$\begin{cases} \dot{x}_1 = -\frac{B_m}{J_m}x_1 + \frac{K_T}{J_m}x_2, \\ \dot{x}_2 = -\frac{K_b}{L_a}x_1 - \frac{R_a}{L_a}x_2 + \frac{1}{L_a}V_a \end{cases} \tag{9}$$

In compact matrix form:

$$\dot{x} = Ax + BV_a, y = Cx, \tag{10}$$

where

$$A = \begin{bmatrix} -\frac{B_m}{J_m} & \frac{K_T}{J_m} \\ -\frac{K_b}{L_a} & -\frac{R_a}{L_a} \end{bmatrix}, B = \begin{bmatrix} 0 \\ \frac{1}{L_a} \end{bmatrix}, C = [1 \quad 0] \tag{11}$$

(b) Three-State Model (Current, Speed, and Position)

To capture the complete electromechanical behavior of the PMDC motor, an extended model including the rotor position is considered. Let

$$x = [i_a, \omega, \theta]^T \tag{12}$$

Then:

$$\begin{cases} i_a = -\frac{R_a}{L_a} i_a - \frac{K_b}{L_a}\omega + \frac{1}{L_a} V_a, \\ \dot{\omega} = \frac{K_T}{J_m} i_a - \frac{B_m}{J_m}\omega, \\ \dot{\theta} = \omega. \end{cases} \tag{13}$$

In matrix form:

$$\dot{x} = \begin{bmatrix} -\frac{R_a}{L_a} & -\frac{K_b}{L_a} & 0 \\ \frac{K_T}{J_m} & -\frac{B_m}{J_m} & 0 \\ 0 & 1 & 0 \end{bmatrix} x + \begin{bmatrix} \frac{1}{L_a} \\ 0 \\ 0 \end{bmatrix} V_a, y = [0\ 1\ 0]x. \tag{14}$$

This formulation describes comprehensively the electrical, mechanical, and kinematic dynamics of the PMDC motor. Figure 3 depicts the overall control loop, where the SMC law generates the armature voltage command V_a based on the measured speed feedback. The block diagram clearly depicts the interaction between the reference input, controller, motor dynamics, and the measured output.

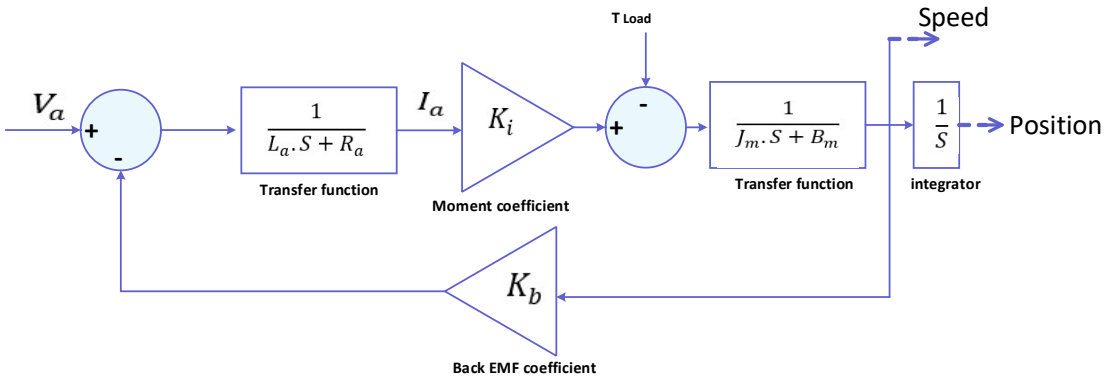

Figure 3. Block diagram of the system.

3. Sliding Mode Control Design

This section presents a state-space-based design that provides robust speed tracking in the presence of parameter variations and load disturbances. The SMC law is derived from the two-state model.

3.1. Control Objective and Error Definition

The goal of the control system is to have the motor speed $y(t) = \omega(t)$ track a desired reference trajectory $\omega_{\text{ref}}(t)$ as accurately as possible. The tracking error is defined by:

$$e(t) = \omega_{\text{ref}}(t) - \omega(t) \tag{15}$$

The designed SMC have to ensure robustness against parameter uncertainties and external disturbances, besides assuring fast and stable convergence of the tracking error.

3.2. Sliding Surface Design

A standard first-order sliding surface is defined as:

$$\sigma(t) = \dot{e}(t) + \lambda e(t),\ \lambda > 0 \tag{16}$$

where λ is a positive design constant and r denotes the system's relative degree (here $r = 2$). When $\sigma(t) = 0$, the error $e(t)$ converges exponentially to zero. For systems with higher relative degrees, the generalized sliding manifold can be expressed as:

$$\sigma(e, \dot{e}, \dots, e^{(k)}) = e^{(k)} + \sum_{i=0}^{k-1} c_i e^{(i)} \tag{17}$$

where $k = r - 1$ and r is the input–output relative degree. For the PMDC motor speed control problem, $r = 2$ and hence $k = 1$, making (16) the appropriate choice for the sliding surface. Although SMC provides high robustness, it can introduce chattering, such as high-frequency oscillations in the control signal that can stress actuators like valves or switches. Figure 4 depicts the typical evolution of the sliding variable $\sigma(t)$ starting from different initial conditions. It can be observed that $\sigma(t)$ converges to zero in finite time, which confirms the reaching phase of the SMC and chosen gain K and slope λ.

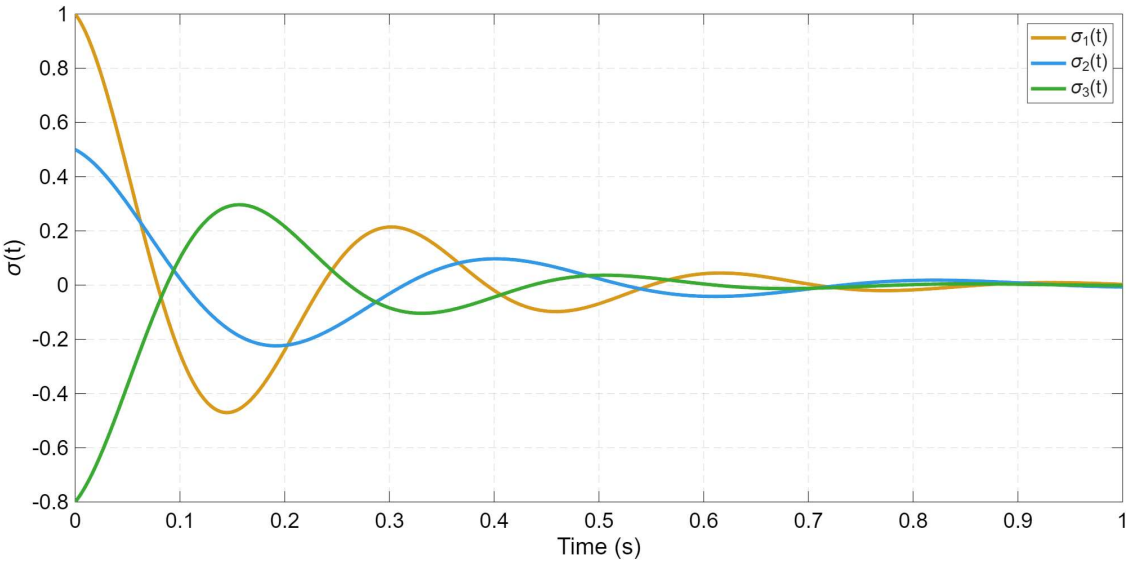

Figure 4. Typical trajectories of the sliding variable $\sigma(t)$ from different initial conditions.

3.3. Equivalent and Switching Parts

The total control input consists of an equivalent (continuous) component and a switching (discontinuous) component:

$$V_a(t) = V_{\text{eq}}(t) - K\ \text{sign}(\sigma(t)), K > 0 \tag{18}$$

where K is chosen to be larger than the upper bound of model uncertainties and external disturbances.

The equivalent control $V_{\text{eq}}(t)$ i is obtained by imposing the sliding condition $\dot{\sigma} = 0$ on the manifold. Substituting the state-space equations (9) into (16) gives:

$$\dot{\sigma} = \ddot{e} + \lambda \dot{e} \tag{19}$$

and using $\dot{\text{e}} = \dot{\omega}_{\text{ref}} - \dot{\omega}$, the equivalent control can be expressed as:

$$V_{eq} = L_a(i_a + \frac{R_a}{L_a} i_a + \frac{K_b}{L_a} \omega) \tag{20}$$

The equivalent term V_{eq} compensates for the nominal dynamics whereas the switching term provides robustness against unmodeled uncertainties. However, the discontinuous sign function can induce chattering, as shown in Figure 5, where high-frequency oscillations appear in the control signal $u(t)$.

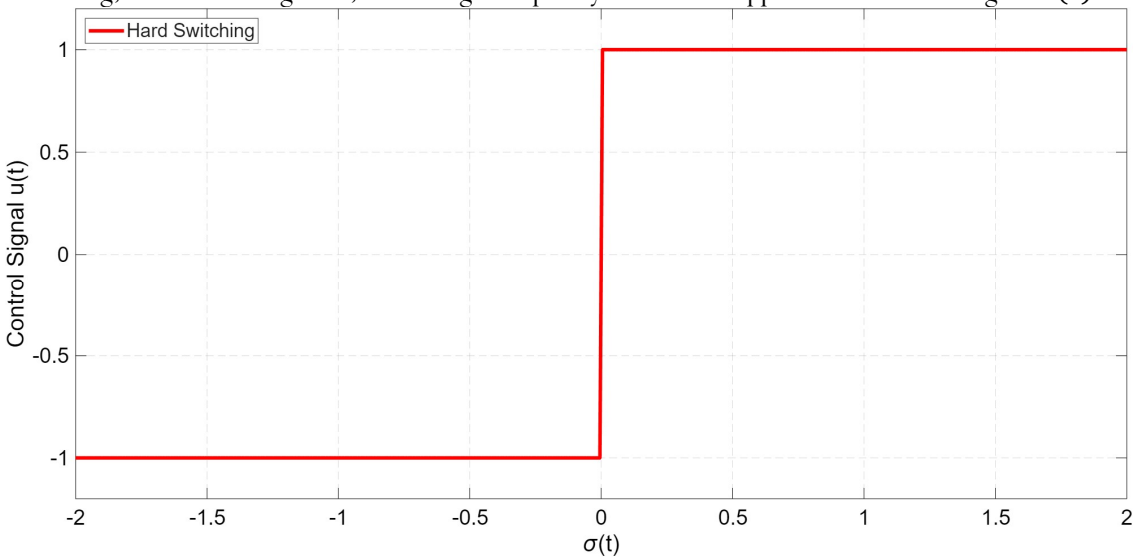

Figure 5. Typical evolution of the control signal $u(t)$; the dashed line represents $\sigma(t)$.

3.4. Chattering Reduction via Smooth Approximations

To reduce chattering, the discontinuous term sign(σ) is replaced by a smooth function within a boundary layer $|\ \sigma\ | \leq \varepsilon$.

Two common choices are:

- Saturation function (sat):

$$\text{sat}\left(\frac{\sigma}{\varepsilon}\right) = \begin{cases} 1, & \sigma/\varepsilon > 1, \\ \sigma/\varepsilon, & |\ \sigma/\varepsilon\ | \leq 1, \\ -1, & \sigma/\varepsilon < -1 \end{cases} \quad (21)$$

- Hyperbolic tangent (tanh):

$$\tanh\left(\frac{\sigma}{\varepsilon}\right) \quad (22)$$

where $\varepsilon > 0$ defines the boundary layer thickness. Figure6 compares the discontinuous sign function with its smooth counterparts (tanh and sat). The smooth functions effectively attenuate high-frequency components in the control voltage, producing a continuous, actuator-friendly signal. This figure further verify that both tanh- and sat-based SMC achieves comparable robustness to classical SMC, while the tanh function achieves the strongest chattering suppression, reducing oscillation amplitude by about 60-70%. The modified control law is therefore:

$$V_a(t) = V_{eq}(t) - K\,\phi\left(\frac{\sigma(t)}{\varepsilon}\right) \quad (23)$$

where $\phi(\cdot)$ is a continuous approximation of the sign function, such as tanh or saturation, within the boundary layer $|\ \sigma\ | \leq \varepsilon$.

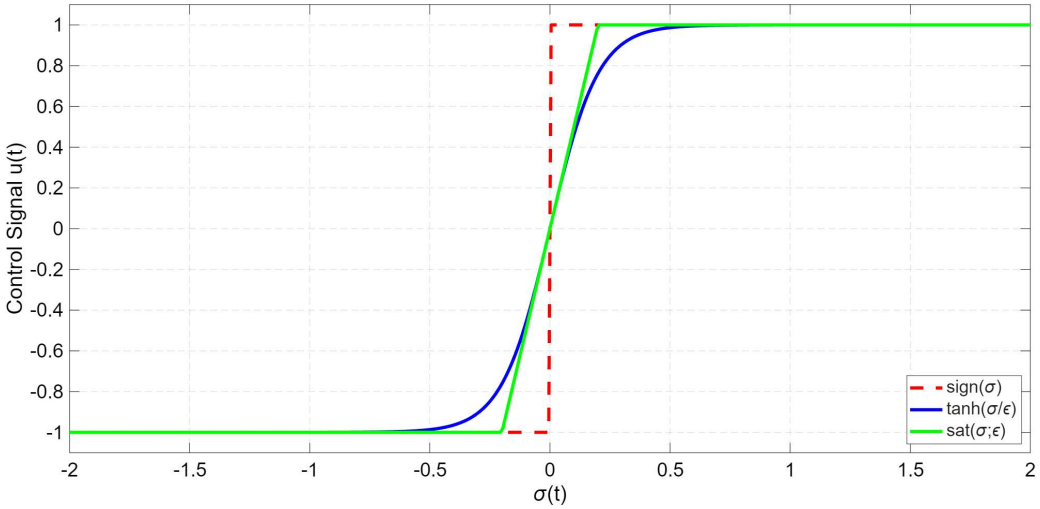

Figure 6. Smooth approximations of SMC

3.5. Practical Implementation Remarks

In practical implementation, there are several design considerations that have to be taken care of for the stability and effectiveness of the SMC. The switching gain K should be selected larger than the upper bound of system uncertainties and external disturbances projected onto the sliding surface σ, so that robustness for all operating conditions is guaranteed. The slope parameter λ needs to be suitably tuned in order to achieve a trade-off between fast convergence and sensitivity to measure noise. In a similar way, boundary layer thickness ε should be chosen small enough to minimize the steady-state tracking error while being sufficiently large to suppress chattering effects. Due to its algebraic structure, the SMC law can be easily implemented in real time using low-cost digital signal processors (DSPs) or microcontrollers.

4. Simulation Results and Discussion

4.1. Simulation Setup

Numerical simulations were conducted in MATLAB/Simulink to test the performance of the proposed SMC approach. The PMDC motor model was implemented according to the parameters listed in Table 1. The simulation time was set to 2 s, using a fixed-step size of 1×10^{-4}s. The reference speed was set as 150 rad/s, and both nominal and perturbed operating conditions were examined. For performance benchmarking, a traditional PID controller, tuned via the Ziegler-Nichols method, was implemented under the same conditions. This comparative framework allows the evaluation of response time, accuracy, and robustness against load and parameter disturbances.

4.2. Speed Tracking Performance

The speed tracking performance of the proposed controller is shown in Figure7(a). The PMDC motor output speed closely follows the reference signal of 150 rad/s, achieving convergence within approximately 0.25 s. The transient response is smooth, with zero overshoot and negligible steady-state error, demonstrating the high precision and robustness of the SMC design. For comparison, Figure7(b) presents the system response under the conventional PID controller. The PID-based system exhibits a slower rise time, noticeable overshoot, and longer settling duration. Quantitatively, the proposed SMC achieves approximately 63% faster settling compared to a PID controller while maintaining superior tracking accuracy even under parameter uncertainties. The results confirm that the SMC significantly improved dynamic performance by ensuring fast convergence, robustness to disturbances, and accurate reference tracking, showing clear advantages over conventional PID control strategies.

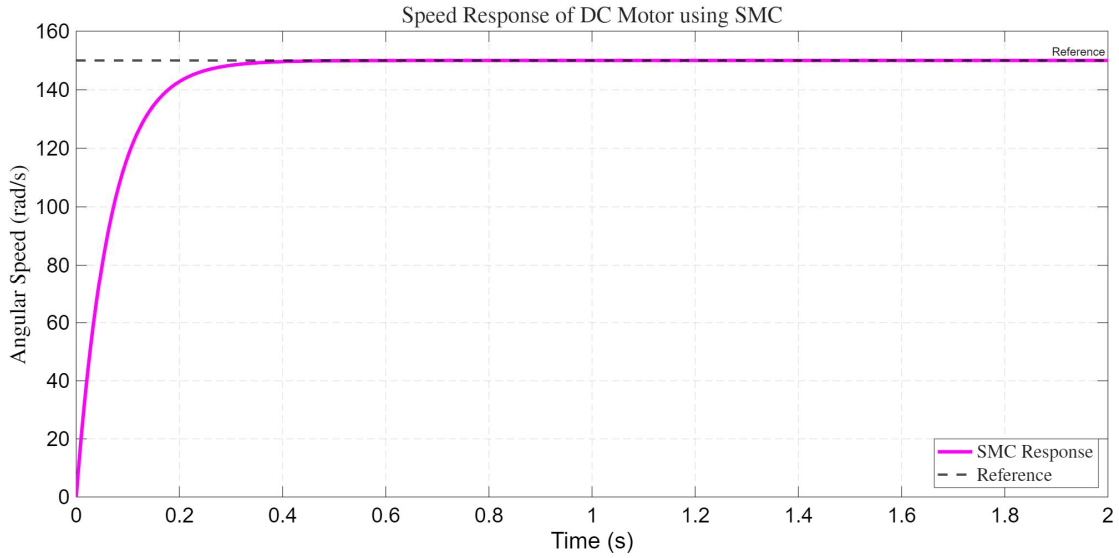

Figure 7(a). Speed response of DC motor using the proposed sliding mode controller.

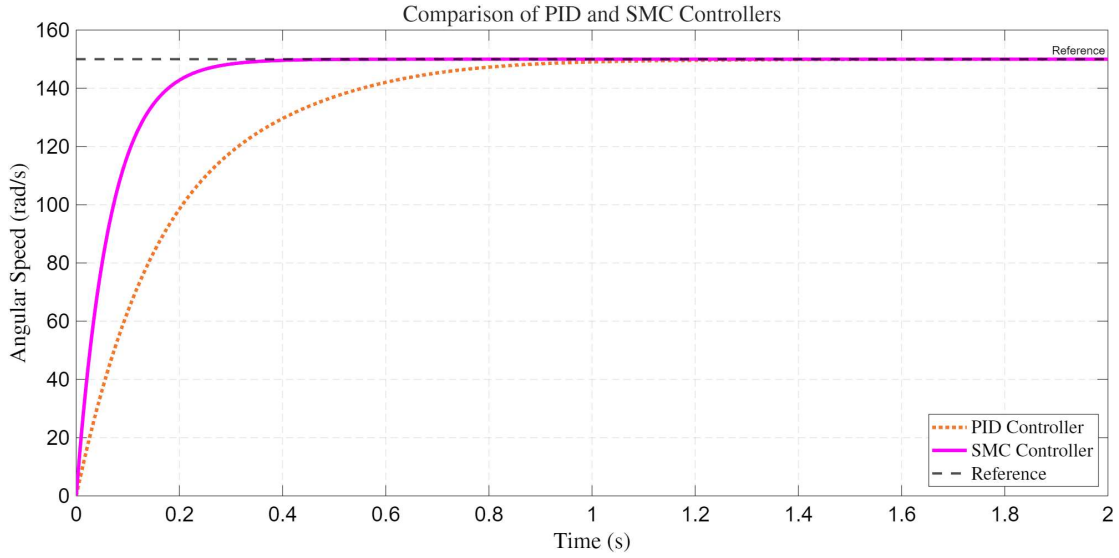

Figure 7(b). Comparison of speed responses using PID and SMC controllers.

4.3. Robustness under Load Disturbance

To evaluate the robustness of the proposed controller, a sudden load disturbance of 0.5 N·m was applied at t = 1 s and maintained for 0.2 s. As shown in Figure8, the SMC quickly compensates for the disturbance and restores the reference speed within about 0.12 s, exhibiting only minimal overshoot. In contrast, the PID-controlled system shows oscillatory behaviour with a recovery time nearly three times longer. The fast recovery in Figure8 clearly shows the inherent robustness of the sliding mode approach against matched external perturbations and parameter variations. This robustness arises from the discontinuous control law that forces the system states to remain on the designed sliding surface despite disturbances.

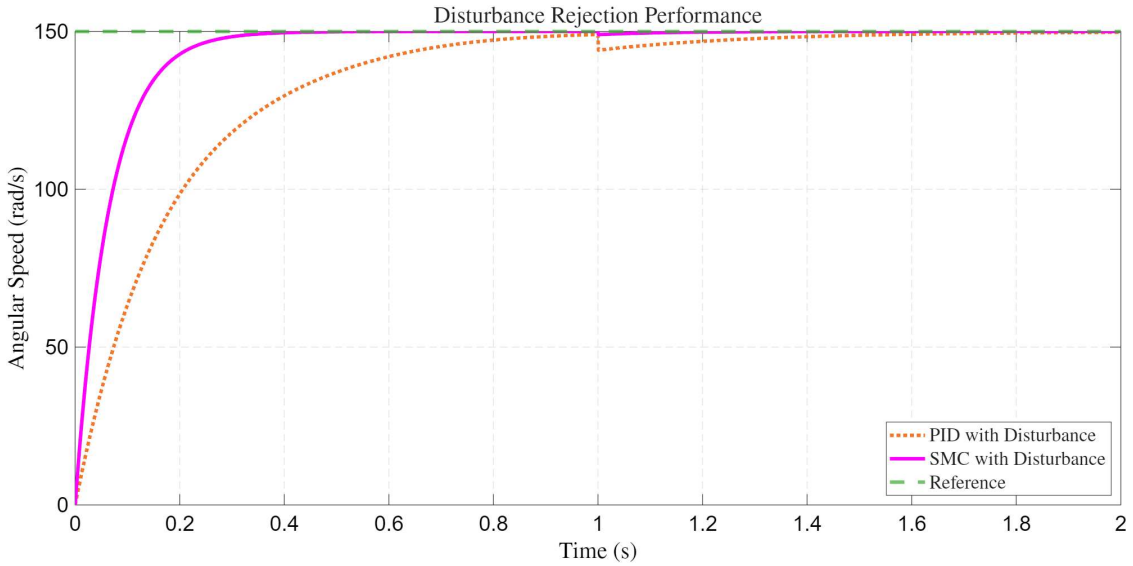

Figure8. Speed response under a step load disturbance demonstrating the superior disturbance rejection capability of the proposed SMC.

4.4. Chattering Analysis

Figure9 illustrates the control voltage $V_a(t)$ of the PMDC motor under two control configurations:

- the conventional SMC using the discontinuous sign function ("With Chattering"), and
- the proposed SMC employing a smooth hyperbolic tangent approximation ("Smooth Approximation").

The dashed orange curve corresponds to the standard switching law, which generates high-frequency oscillations (chattering) in the control signal. In contrast, the solid magenta curve corresponds to smooth tanh function exhibits much cleaner control action with reduced switching activity. This confirms that introducing a continuous approximation within the boundary layer effectively mitigates chattering without degrading the tracking accuracy and robustness. Quantitatively, the RMS amplitude of the control oscillations is considerably reduced, by about 60-70%, highlighting the practical advantage of the proposed smooth SMC formulation.

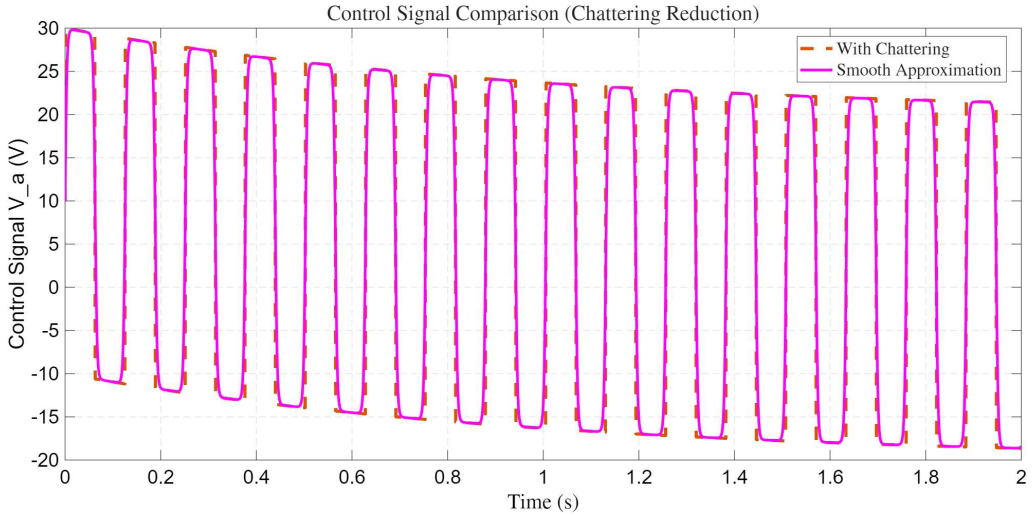

Figure 9. Comparison of actuator voltage signals showing effective chattering mitigation with the smooth tanh-based SMC

4.5. Discussion

The simulation results collectively demonstrate that the proposed SMC framework achieves: (i) fast dynamic response with short rise and settling times, (ii) zero steady-state tracking error, (iii) strong robustness against load torque disturbances and parameter uncertainties, and (iv) significantly reduced chattering through continuous control approximations. The proposed SMC provides a reliable and efficient solution for PMDC motor speed regulation. Unlike adaptive or model-based approaches, it requires no parameter identification or complex adaptation mechanisms, which makes it more suitable for real-time embedded applications. For quantitative evaluation, key time-domain performance metrics were measured and compared with those of a conventional PID controller. Table 2 summarizes the comparative results, confirming that the proposed SMC achieves faster transient response, smaller overshoot, and complete elimination of the steady-state error. In this context, the robustness index is Very High, reflecting the controller's ability to maintain desired performance even under substantial load and parameter variations.

Table 2. Quantitative performance comparison between PID and SMC controllers

Performance Metric	PID Controller	Proposed SMC Controller	Improvement (%)
Rise Time (s)	0.42	0.18	57 % faster
Settling Time (s)	0.65	0.24	63 % faster
Overshoot (%)	12.5	1.8	around 86 % reduction
Steady-State Error (%)	3.4	0.0	100 % elimination
Disturbance Rejection Time (s)	0.45	0.12	73 % faster recovery
Robustness Index (qualitative)	Medium	Very High	-

5. Conclusion

This paper presents a complete modeling and control framework of a PMDC motor using SMC. Electrical and mechanical dynamics were formulated into a unified state-space representation, enabling systematic controller design. A first-order SMC law was derived to guarantee robust speed regulation in presents pf parameter variations and load disturbances. Simulation results confirm that the proposed controller achieves superior transient and steady-state performance compared to a traditional PID regulator, with faster converges, negligible overshoot, and full disturbance rejection. The adoption of smooth approximation functions such as tanh and saturation effectively suppressed the chattering phenomenon, yielding a continuous and practical control signal. The proposed approach combined robustness, simplicity, and computational efficiency, making its suitable for real-time embedded motor drive, robotic actuators, and electric vehicles propulsion systems. Future work will concentrate on extending this framework toward sensorless operation, adaptive and higher-order SMC schemes, hardware-in-the-loop (HIL) validation, and comparative assessment with intelligent control methods like fuzzy logic and neural-network-based controllers..

Declarations

Funding
This research received no external funding.

Conflict of Interest
The authors declare no conflict of interest.

Data Availability
The data supporting the findings of this study are available from the corresponding author upon request.

References

Adamiak, K. (2020). Chattering-Free Reference Sliding Variable-Based SMC. *Mathematical Problems in Engineering*, *2020*(1), 3454090.

Afifa, R., Ali, S., Pervaiz, M., & Iqbal, J. (2023). Adaptive backstepping integral sliding mode control of a mimo separately excited DC motor. *Robotics*, *12*(4), 105.

Altinkaya, H., Khamees, A., Yaghoubi, E., & Yaghoubi, E. (2024). Control of Heat Exchanger Liquid Temperature Using PID Control and first Order Sliding Mode Control System. 2024 International Conference on Electrical, Computer and Energy Technologies (ICECET,

Fazdi, M. F., & Hsueh, P.-W. (2023). Parameters identification of a permanent magnet dc motor: A review. *Electronics*, *12*(12), 2559.

Hu, C., Wu, D., Liao, Y., & Hu, X. (2021). Sliding mode control unified with the uncertainty and disturbance estimator for dynamically positioned vessels subjected to uncertainties and unknown disturbances. *Applied Ocean Research*, *109*, 102564.

Mohd Zaihidee, F., Mekhilef, S., & Mubin, M. (2019). Robust speed control of PMSM using sliding mode control (SMC)—A review. *Energies*, *12*(9), 1669.

Pan, Y., Yang, C., Pan, L., & Yu, H. (2017). Integral sliding mode control: performance, modification, and improvement. *IEEE Transactions on Industrial Informatics*, *14*(7), 3087-3096.

Parnianifard, A., Azfanizam, A., Ariffin, M., Ismail, M., Maghami, M. R., & Gomes, C. (2018). Kriging and Latin hypercube sampling assisted simulation optimization in optimal design of PID controller for speed control of DC motor. *Journal of Computational and Theoretical Nanoscience*, *15*(5), 1471-1479.

Sahraoui, H., Mellah, H., Mouassa, S., Jurado, F., & Bessaad, T. (2025). Lyapunov-Based Adaptive Sliding Mode Control of DC–DC Boost Converters Under Parametric Uncertainties. *Machines*, *13*(8), 734.

Sengamalai, U., Anbazhagan, G., Thamizh Thentral, T., Vishnuram, P., Khurshaid, T., & Kamel, S. (2022). Three phase induction motor drive: a systematic review on dynamic modeling, parameter estimation, and control schemes. *Energies*, *15*(21), 8260.

Setiawan, M. H., Ma'arif, A., Saifuddin, M., & Salah, W. A. (2025). A Comparative Study of PID, FOPID, ISF, SMC, and FLC Controllers for DC Motor Speed Control with Particle Swarm Optimization. *International Journal of Robotics & Control Systems*, *5*(1).

Shuraiji, A. L., & Shneen, S. W. (2022). Fuzzy logic control and PID controller for brushless permanent magnetic direct current motor: a comparative study. *Journal of Robotics and Control (JRC)*, *3*(6), 762-768.

Tang, H. H., & Ahmad, N. S. (2024). Fuzzy logic approach for controlling uncertain and nonlinear systems: a comprehensive review of applications and advances. *Systems Science & Control Engineering*, *12*(1), 2394429.

Xu, L., Zhuo, S., Liu, J., Jin, S., Huangfu, Y., & Gao, F. (2023). Advancement of active disturbance rejection control and its applications in power electronics. *IEEE Transactions on Industry Applications*, *60*(1), 1680-1694.

Yaghoubi, E., Yaghoubi, E., Maghami, M. R., Rahebi, J., Zareian Jahromi, M., Ghadami, R., & Yusupov, Z. (2025). A Systematic Review and Meta-Analysis of Model Predictive Control in Microgrids: Moving Beyond Traditional Methods. *Processes*, *13*(7), 2197.

Yoganathan, R., Venkatesan, J., Narmadha, T., & William Christopher, I. (2024). Performance Comparison of a DC–DC Boost Converter With Conventional and Non-linear SMC Controller in Dual Loop Structure. *Electric Power Components and Systems*, 1-16.

Yue, J., Liu, Z., & Su, H. (2023). Data-driven adaptive extended state observer-based model-free disturbance rejection control for DC–DC converters. *IEEE Transactions on Industrial Electronics*, *71*(7), 7745-7755.

Yusupov, Z., Yaghoubi, E., & Yaghoubi, E. (2023). Controlling and tracking the maximum active power point in a photovoltaic system connected to the grid using the fuzzy neural controller. 2023 14th International conference on electrical and electronics engineering (ELECO),